ADVANCES IN MATERIALS SCIENCE, Vol. 18, No. 3 (57), September 2018

sciendo

DOI: 10.1515/adms-2017-0039

L. Tuz

AGH University of Science and Technology in Krakow, Faculty Metals Engineering and Industrial Computer Science, Department of Physical Metallurgy & Powder Metallurgy, Poland
ltuz@agh.edu.pl

EVALUATION OF MICROSTRUCTURE AND SELECTED MECHANICAL PROPERTIES OF LASER BEAM WELDED S690QL HIGH-STRENGTH STEEL

ABSTRACT

The paper presents results of microstructure and mechanical properties investigation of laser beam welded high-strength steel. Material for test was non-alloyed steel with yield strength of 690 MPa after quenching and tempering in delivery condition. Research carried out on the butt-welded joints shows fine-grain martensitic-bainitic structure of base metal and in the weld. Investigations of mechanical properties revealed the softened zone in HAZ where the hardness decrease without microstructural changes was observed. Moreover, an influence of softened zone and HAZ width on impact strength was observed where the occurrence of lower hardness led to fracture path deviation phenomenon.

Keywords: *high-strength steel, microstructure, laser welding*

INTRODUCTION

Recently, different grades of high-strength steel are constantly gaining popularity in various branches of industry. This is the result of, on the one hand, the necessity of limiting the mass of final products, and on the other hand, obtaining the highest possible strength to mass or plasticity to mass ratio while limiting the use of expensive alloying elements. Weight reduction is associated with many factors regarding the reduction of material consumption, energy consumption in production and operation, and the disposal of products [1]. The steel manufacturers' response to this demand is constantly improved by heat treatment, where a relatively simple chemical composition through controlled rolling combined with heating and cooling of steel (quenching and tempering) yields high mechanical properties and plasticity [2, 4]. Among the available structural unalloyed steels, a yield strength of up to 1300 MPa and with an elongation of up to 10% is obtained as a result of heat treatment. In addition, these materials are also characterized by relatively high impact strength at low temperatures (even in -60°C) [5-7].

The high strength of the steel enables the optimization of the wall thickness, and thus also the thickness of the welds, at the design stage of the structure [7]. The ability to carry out a convenient selection of wall thickness is important for many industries, where high-strength steels are used, e.g. in the power industry [8] or for the construction of gas-transmission pipe lines [9]. For materials used in these areas, often strict requirements are applied to obtain the appropriate maximum hardness in the area of the welded joint. In the case of non-alloy heat-treated structural steels, it is crucial that the hardness does not decrease due to the heat input during welding [5, 8, 9, 10].

Due to the manufacturing process involving combined rolling and thermal improvement, these materials are sensitive to the effects of heat input during eg welding. This causes that it is necessary to use the appropriate linear energy (heat input) ensuring proper penetration, but at the same time limiting the width of the heat affected zone (HAZ). In the heat-affected zone, grain growth may occur at high temperature HAZ or tempering of steel in the low-temperature area of HAZ. These phenomena are particularly observed in arc welding processes, where a relatively large diameter weld pool is formed and a large amount of heat input is due to the low welding speed [4, 11, 12]. The solution is to automate welding processes, e.g. by robotization, where it is possible to increase the welding speed up to 1.5 m/min. Another method is the use of advanced welding technologies such as laser beam welding or plasma arc welding. The use of these methods allows on the one hand an increase in welding speed of up to 3 m/min and obtaining a narrow joint and HAZ. Hence, the paper attempts to make butt welds of high strength steel S690QL and the quality assessment of welded joints based on the evaluation of the microstructure and selected mechanical properties.

EXPERIMENTAL

The test material was butt welded flat plates with dimensions 3x120x60 mm made of high-strength quenched and tempered steel grade S690QL. The joints were made using a laser beam (IPG Photonics fiber laser) with a power of 3 kW and with a welding velocity of 2.5 m/min (0.041 m/s). Welding process were carried out without filler metal. The focal diameter was 0.6 mm. The chemical composition determined by the use of optical emission spectroscopy and selected mechanical properties of steel according inspection certificate 3.1 acc to EN 10204 are given in Table 1, what is confirmation of EN ISO 10025-6 requirements.

Table 1. *Chemical composition and selected mechanical properties of S690QL steel*

<table>
<tr><td colspan="14">Chemical composition, wt.%</td></tr>
<tr><td>C</td><td>Si</td><td>Mn</td><td>P</td><td>S</td><td>Al</td><td>B</td><td>Cr</td><td>Cu</td><td>Mo</td><td>N</td><td>Nb</td><td>Ni</td><td>Ti</td></tr>
<tr><td>0.14</td><td>0.2</td><td>1.15</td><td>0.009</td><td>0.002</td><td>0.079</td><td>0.0024</td><td>0.33</td><td>0.02</td><td>0.3</td><td>0.005</td><td>0.029</td><td>0.04</td><td>0.004</td></tr>
<tr><td colspan="14">Mechanical properties</td></tr>
<tr><td colspan="6">Tensile strength (R_m), MPa</td><td colspan="2">Elongation (A), %</td><td colspan="6">Impact strength, J/cm^2</td></tr>
<tr><td colspan="6" rowspan="2">882</td><td colspan="2" rowspan="2">15</td><td colspan="3">Temp. -40°C</td><td colspan="3">Temp. -60°C</td></tr>
<tr><td colspan="3">159</td><td colspan="3">130</td></tr>
</table>

Based on the established chemical composition, the carbon equivalent of Ce = 0.462% was determined according to the formula (1).

$$Ce = C + \frac{Mn}{6} + \frac{Cr + Mo + V}{5} + \frac{Ni + Cu}{15} = 0.462\% \tag{1}$$

The value of the determined carbon equivalent indicates that the tested steel is characterized by good weldability and does not require additional technological operations in the welding process.

METHODOLOGY

Samples for testing were cut with a circular saw with intensive cooling to avoid the impact of cutting temperature on structure changes. Such cut samples were mounted in an epoxy resin and ground on aqueous abrasive papers with increasing granularity from 100 to 1000 for macroscopic studies and up to 1500 for microscopic examinations. Samples for microscopic observations were subjected to a polishing process on a polishing cloth using an aqueous suspension of aluminum oxide. The metallographic samples thus prepared were subjected to etching in Adler's reagent in macroscopic studies and 4% alcoholic solution of nitric acid (nital). Structural observations were carried out using light microscopy and scanning electron microscopy.

The tests of mechanical properties included measurements of Vickers hardness with a load of 0.5 kG indenter, impact test and three-point bending test. Hardness measurements were carried out along the measuring line on the cross-section of the welded joint, making indentation every 0.2 mm. The three-point bending test was carried out on the face and root sides using 30 mm diameter supports on 15x80 mm samples without grinding face and root of weld. Investigations of Charpy impact strength of welded joints were carried out on thinned samples with dimensions of 2.5x10x55 mm with V-notch cut in the weld.

RESULTS

Macroscopic examination

Figure 1 presents the macrostructure of the welded joint observed on the cross-section of the weld axis. The joint has a regular shape with a visible slight narrowing in the middle of the sheet thickness. The width of face and root is similar and amounts to approx. 1 mm. The width of the heat affected zone (HAZ) is uniform throughout the thickness of the welded joint and does not exceed 0.5 mm. Welded joints are characterized by the presence of slight reinforcement on the face side (about 0.07 mm) and slightly concave root (about 0.06 mm).

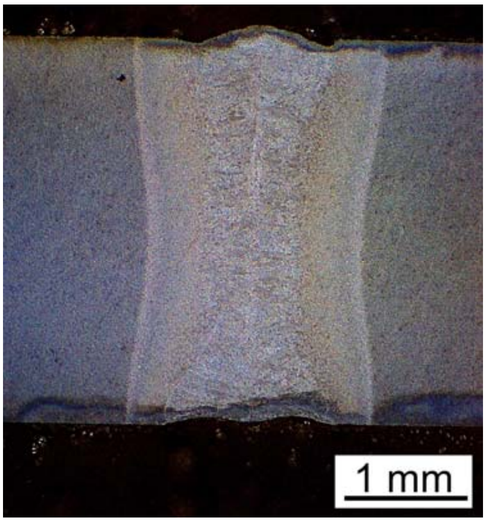

Fig. 1. Macrostructure of S690QL laser beam butt welded joint

Microscopic examination

The base material is characterized by a fine-grained martensitic-bainitic structure and a structure of tempered martensite. Figure 2 presents the structure observed using light microscopy and scanning electron microscopy. In the observed structure, the visible grain boundaries are the effect of the steel tempering process.

a) b)

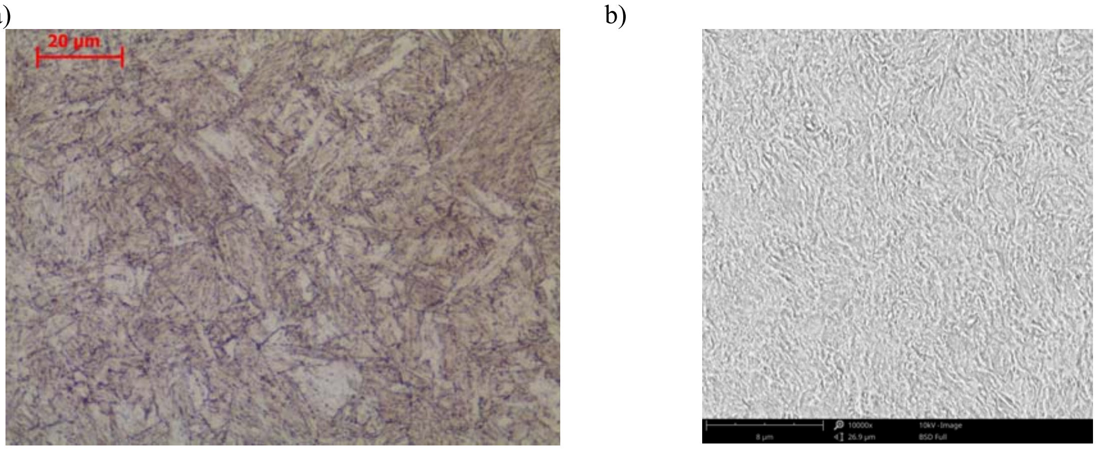

Fig. 2. Microstructure of base material. Fine-grained martensitic-bainitic structure: a) light microscopy, magnitude 1000x, b) scanning electron microscopy, magnitude 10.000x

In the area of HAZ, the occurrence of characteristic structures being the effect of the heat input from the welding process was observed. Just behind the base material there is a intercritical zone heated during welding to the temperature in the Ac_1-Ac_3 range. The structure has the character of tempered martensite with visible areas of granular ferrite (Fig. 3).

Further towards the fusion line, the fine-grain zone was heated to a temperature in the range of Ac_3-1100°C. It is characterized by a fine-grained, tempered bainitic-martensitic structure (Fig. 4). Near the fusion line, there is an overheating area with a coarse bainitic-martensitic structure (Fig. 5).

The weld is characterized by a coarse structure with a characteristic arrangement of crystallites in the direction of heat dissipation. Due to the high cooling rate of the weld, which is the effect of heat removal to the adjacent material, the structure of column crystals arranged in parallel and touching vertices in the weld axis is observed. Inside the crystallites, a lath martensitic structure and a martensitic-bainitic structure is observed (Fig. 6).

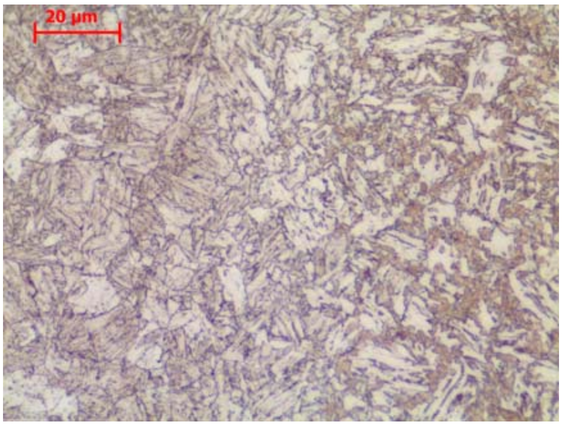

Fig. 3. Microstructure in the area of intercritical HAZ

a) b)

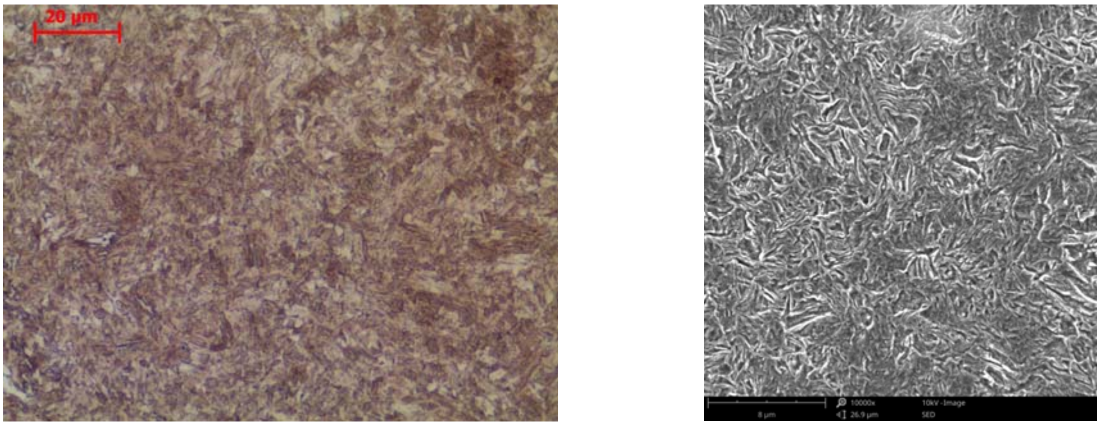

Fig. 4. Microstructure in the area of fine-grain HAZ; a) LM image, b) SEM image

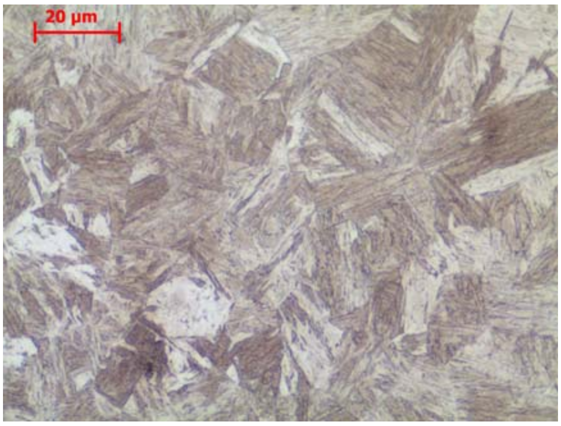

Fig. 5. Microstructure in the area of the grain growth zone (coarse-grain HAZ)

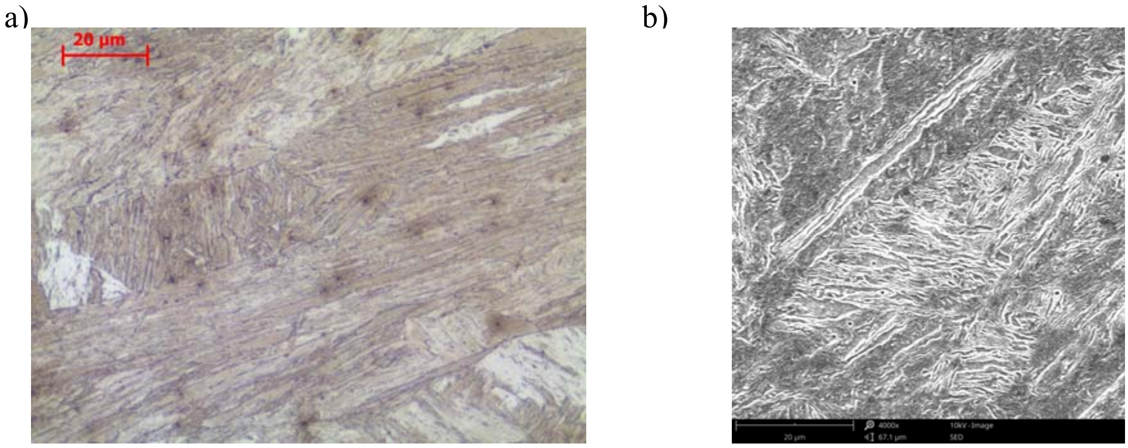

Fig. 6. Weld microstructure. Coarse crystalline structure with visible martensite lath

Bending test

The bending test was carried out to identify the tendency to crack during deformation due to the presence of weld imperfections in the area of the face and root of the weld (reinforcement on the face side and concave of the root). The test was carried out using the three-point lateral bending method with the bending mandrel. Samples were bent both from the faces and the roots. In all cases, a bending angle of 160 ° without cracks was reached, which indicates the good plastic properties of the welded joint. Table 2 summarizes the results of the bending test.

Table 2. *Results of bending test*

Specimen number	Max bending force, N	Tension area	Bending angle	Final result
1_L	2.400	Face of weld	Over 160°	No cracks
2_L	2.360	Face of weld	Over 160°	No cracks
3_G	2.380	Root of weld	Over 160°	No cracks
4_G	2.400	Root of weld	Over 160°	No cracks

Impact test

Impact tests were carried out using a Charpy hammer weighing 15 kg. The impact test consists in breaking the specimen with V notched of 2 mm depth and the radius of the tip rounding of 0.25 mm. The result of the test is the amount of energy absorbed to break the sample or its ratio to the cross-sectional area of the sample at the notch location. The test was carried out on samples with dimensions of 2.5x10x55 mm. Samples with dimensions of 2.5x10x55 mm were taken from the area of the weld joint in such a way that the notch is in the weld. The samples revealed the plastic fracture. The performed tests indicate high impact strength of the weld (table 6). Observations of samples after testing revealed, that the fracture does not follow the weld (Fig. 7a). It is initiated in the bottom of the notch, but deviates further in the direction of HAZ and continues in this area or in base metal (Fig. 7b). This behavior should be attributed to the crack propagation through the zone with the lowest hardness. In heat-treated steels, the area with the lowest hardness is located just behind the HAZ or heated to a temperature below Ac1.

a) b)

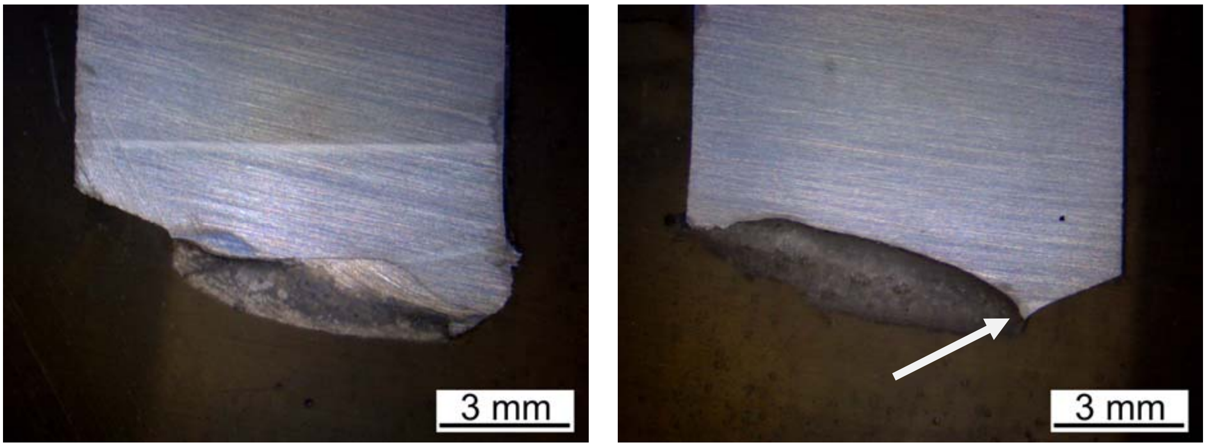

Fig. 7. Impact test: a) macrostructure after the impact test, visible notch bottom and the course of the crack initially along the HAZ boundary b) the course of the crack initiated in the bottom of the notch and its deviation into the base material

Table 6. *Results of impact test. V-notch in the weld area*

Sample no	Impact energy [J]	Impact strength [J/cm^2]*
1	177	221
2	196	245
3	186	233
4	226	282

*The impact strength and energy calculated for sample with dimensions 10x10x55 mm.

Microhardness

Vickers microhardness measurements at 0.5 kG indent load were made on the cross section of the welded joint along the measurement line. The results are shown in Figure 8. The hardness distribution indicates an uneven hardness distribution with a joint area where the highest hardness values exceeding 450 HV were recorded in HAZ, indicating that this area may have a tendency to brittle fracture. In the joint, the hardness ranges from 394 HV to 423 HV. In addition, the occurrence of a narrow softening zone at the border of the HAZ and base material was observed. This zone is relatively narrow, which may indicate that there will be no loss of mechanical properties in this area due to the contact reinforcement under the influence of static tensile forces. This area is characterized by the lowest hardness in the whole welded joint (297-300 HV), which means that in the case of impact in this area, a crack will occur, which was confirmed by impact tests.

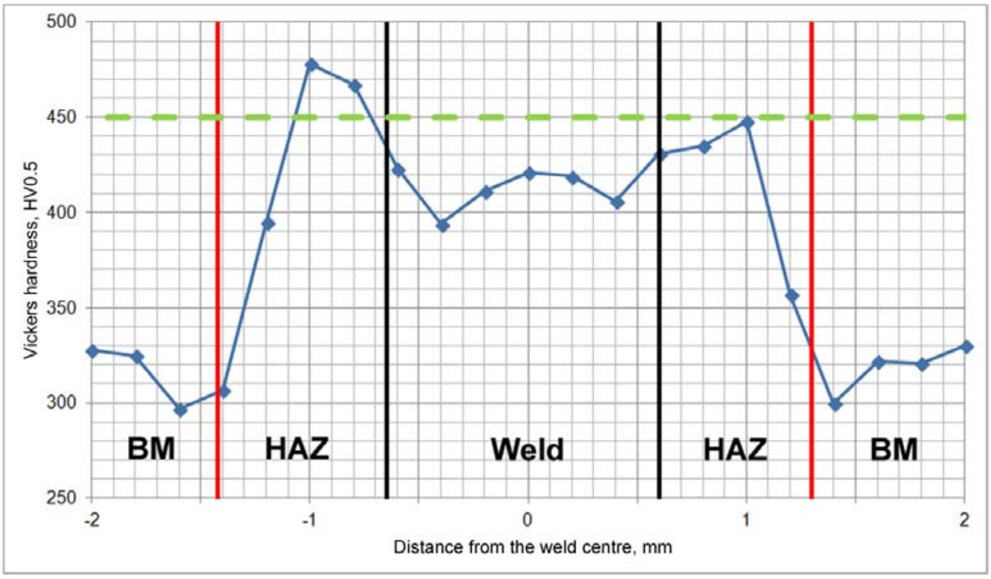

Fig. 8. Vickers hardness distribution in cross section of butt weld (HV0.5)

CONCLUSIONS

The following conclusions were made on the basis of the conducted research:

- in the laser welded joint without the addition of filler material there may be welding imperfections in the area of face and root of welds of insignificant dimensions, which are not detectable in visual tests (NDT), but only in macroscopic tests (DT). As shown by the bending test, the presence of these shape errors does not cause cracks to initiate during the static loading due to the high plasticity of the entire joint,
- in the area of the entire joint a bainite-martensitic structure is observed, in the parent material it is a fine-grained structure, and in the weld has the structure of column crystals touching the ends of the weld axis, only a slight grain growth is observed in the heat affected zone in the superheat area,
- the weld is characterized by high impact strength, while during the measurements due to the narrow joint (less than 1 mm) the crack initiated at the bottom of the notch tends to diverge and continues through the zone with the lowest hardness (FDP mechanism),
- high welding speed and relatively high linear welding energy affect a strong increase in hardness in HAZ (above 450 HV) due to the heat being taken away by the cold base material; in the weld, an increase of approx. 100 HV is observed in relation to the parent material,
- between the parent material (heated up below Ac1) and HAZ in the narrow area, a drop in hardness to approx. 300 HV is observed - the softening zone.

REFERENCES

1. Goss C., Marecki P., Applications of high strength steels in welded structures on the example of XABO 890 and XABO 960 steels, [Zastosowanie stali wysokowytrzymałych w konstrukcjach spawanych na przykładzie stali XABO 890 i XABO 960]; Logistyka, 6 (2014), p. 4122-4129. (In Polish).

2. Brezová B., Mäsiar H., Radič P., Welding of high strength materials used in the manufacture of special equipment, University Review, 8, 3-4 (2014), 51-61.

3. Löbbe Ch., Hering O., Hiegemann L., Tekkaya A.E., Setting mechanical properties of high strength steels for rapid hot forming processes, Materials, 9 (2016), 229 doi:10.3390/ma9040229.

4. Banerjee K., Improving weldability of an advanced high strength steel by design of base metal microstructure; Journal of Materials Processing Technology, 229 (2016), 596–608.

5. Nowacki J., Sajek A., Matkowski P., The influence of welding heat input on the microstructure of joints of S1100QL steel in one-pass welding; Archives of Civil and Mechanical Engineering, 16 (2016), 777–783.

6. Barsoum Z., Khurshid M., Ultimate strength of welded joints in high strength steels, Procedia Structural Integrity, 5 (2017), 1401-1408.

7. K. Pańcikiewicz, L. Tuz, Z. Żurek, Ł. Rakoczy; Optimization of filler metals consumption in the production of welded steel structures; Advanced in Materials Science, 16(1) (2016), p. 27-34; doi: 10.1515/adms-2016-0003

8. Pańcikiewicz K., Zielińska-Lipiec A., Tasak E., Cracking of high-strength steel welded joints; Advanced in Materials Science, 13(3) (2013), 76-85; doi: 10.2478/adms-2013-0013.

9. Rogalski G., Fydrych D., Łabanowski J., Underwater Wet Repair Welding of API 5L X65M Pipeline Steel, Polish Maritime Research, 24 1 (93) (2017), 188-194; doi: 10.1515/pomr-2017-0038.

10. Świerczyńska A., Fydrych D., Rogalski G., Diffusible hydrogen management in underwater wet self-shielded flux cored arc welding, International Journal of Hydrogen Energy, 42(38) (2017), 24532-24540.

11. Kurc-Lisiecka A., Lisiecki A., Laser welding of the new grade of advanced high-strength steel Domex 960, Materiali in tehnologije / Materials and technology, 51(2) (2017), 199–204; doi:10.17222/mit.2015.158.

12. Kurc-Lisiecka A., Piwnik J., Lisiecki A., Laser welding of new grade of advanced high strength steel STRENX 1100 MC, Archives of Metallurgy Materials, 62(3) (2017), 1651-1657; doi: 10.1515/amm-2017-0253.